Final Report

on

A FEASIBILITY STUDY OF THE PRODUCTION OF LOW LOSS IR FIBERS IN SPACE

prepared for

Defense Advanced Research Projects Agency

by

Michael C. Weinberg, George F. Neilson and Michail A. Zak

Jet Propulsion Laboratory
Applied Mechanics Division
4800 Oak Grove Drive
Pasadena, California 91109

November 15, 1983

Final Report

on

A FEASIBILITY STUDY OF THE PRODUCTION OF LOW LOSS IR FIBERS IN SPACE

prepared for

Defense Advanced Research Projects Agency

NASA Contract NAS7-918

by

Michael C. Weinberg, George F. Neilson and Michail A. Zak

AO 4665

Agent = NASA #NAS7-918

Jet Propulsion Laboratory
Applied Mechanics Division
4800 Oak Grove Drive
Pasadena, California 91109

November 15, 1983

ABSTRACT

In this study a preliminary evaluation is made of the feasibility of preparing fluoride glass optical fibers in space. The glass processing steps are analyzed and those which may contribute to property degradation are indicated, and the possibility of successfully executing such steps in space are considered.

Two critical factors are the relative cooling rates and fluid flow characteristics of the fibers, during drawing, on earth and in space. It has been concluded that fiber cooling rates in space will be equal to or less than those on earth. This feature is detrimental to fiber pulling in space. Also, gravity plays a small role in determining the characteristics of the fluid flow. However, at higher temperatures, where the viscosity is low, gravitational effects could be important in determining the pulling force on the fiber, and it is believed that certain flows unobtainable on earth could be realized in space. This flow regime could potentially be utilized advantageously for the production of fluoride fibers in space. However, additional calculations and experiments are required to demonstrate the feasibility of this approach.

TABLE OF CONTENTS

I. Introduction.....1

II. Analysis of Ground-Based Processing of Fluoride Glass Fibers.....3

III. Potential Advantages of Space Processing of Fluoride Glass Fibers.....11

IV. Evaluation of the Advantages and Problems Associated with Fluoride Glass Fiber Production in Space.....15

V. Required Ground-Based Experimentation.....32

VI. Required Computations and Modelling.....36

VII. Summary.....39

Appendix A.....41

References.....43

Figure Captions.....45

Figures.....46

I. Introduction

During the past two decades tremendous progress has been made in the development of low loss silica optical fibers. However, further significant improvement in loss reduction is not anticipated for such fibers since the theoretical minimum loss is being approached.

On the other hand, the newly discovered class of heavy metal fluoride glasses (1, 2) have potential losses 2 to 3 orders of magnitude lower than silica fibers. Projections of loss which have been made for typical fluoride glasses, based upon the intersection of the multiphonon absorption edge and Rayleigh scattering curves, indicate potential losses as low as 10^{-3} db/km at 3.5μ (3). Yet, to date, all fluoride glass fibers which have been produced have exhibited substantially higher losses. The origin of these losses are due to foreign ion absorptions, water, and microinclusions (crystallites). Thus, to realize the full potential of fluoride glasses for optical fiber applications these processing problems must be surmounted.

The basic objective of this study is to assess whether any of these processing difficulties may be overcome by preparing fluoride glass optical fibers in space. In performing this assessment the following items are presented.

In Section II an analysis is given of the ground-based processing sequence used to produce fluoride fibers, including an examination of those steps which may lead to property degradation due to crystallite formation or phase separation in the glass.

A discussion of the possible methods which may allow for a successful execution of the above steps in space is presented in Section III.

In Section IV a preliminary evaluation is given of the relative advantages and unique problems which may be associated with the production of fluoride glass fibers in space.

In Sections V and VI descriptions are given of the required experimental and mathematical modelling studies, respectively, which should be performed to confirm our preliminary findings.

II. Analysis of Ground-Based Processing of Fluoride Fibers

A large number of factors could affect the ability to produce fluoride glass fibers free of crystallites or phase separated regions. Such factors could be inherent to the choice of glass composition, the glass preparation procedure, or the fiber drawing method.

Choice of the fluoride glass to be used as an optical fiber is very critical since the glass must simultaneously satisfy a large number of requirements. These requirements relate to the optical and mechanical properties of the glass, the glass durability, and the glass stability and workability. In many instances changes in composition which tend to improve the glass with respect to one desired property, degrade it with respect to another. For example, it has been noted that addition of small amounts of AlF_3 tends to stabilize the base glass composition (4). However, AlF_3 additions increase multiphonon absorption, and hence degrade IR transparency in the regime of interest (4). Thus, the optimization of fluoride glass composition for employment as fiber optic material is a very difficult task because of the conflicting requirements imposed.

If one foregoes the quest for the ideal composition, then it appears reasonable to initially relax the requirements on the optical and mechanical properties, and focus on the question of glass purity and stability. The rationale for this approach is as follows. Nearly any of the myriad of compositions investigated to date have theoretical losses far better than silicate fibers. However, the

actual losses which have been measured in fibers are orders of magnitude larger than the theoretical losses. These losses stem from trace amounts of transition metal ion impurities and micro-inclusions in the glass. Thus, choosing a glass composition in which the latter may be minimized is a much more important task at this juncture than optimizing the glass composition in light of predicted theoretical loss behavior.

Thus, an important question that should be addressed is: which compositions are good glass formers? (i.e., form readily and are not prone to devitrification or phase separation.) The general question of glass formation has recently been reviewed by Uhlmann (5). He discusses three approaches to glass formation: structural approaches, thermodynamic approaches, and kinetic approaches. Uhlmann has indicated that the structural approach based on Zachariasen's Rules for glass formation are inadequate even for predicting oxide glass formation. Moreover, it has been observed that this approach is totally inadequate to explain fluoride glass formation (4). Uhlmann has argued that the thermodynamic approaches, also, have proven inadequate to describe glass formation ability. The kinetic approaches to glass formation focus on the calculation of crystallization rates in potential glass forming systems. For a given cooling rate of the melt, if crystallization does not occur then glass formation will eventually ensue. This method of predicting glass formation has been employed by Turnbull (6) and Uhlmann and coworkers (7-9). Unfortunately, this method has a number of severe limitations too. It is most easily applicable only to single component or congruently melting systems. Also, to employ the theory one must have knowledge of several physical parameters some of which are difficult to

determine (e.g., the liquid-crystal surface tension). Finally, the theory rests upon the validity of classical nucleation theory. However, the validity of this theory with respect to crystal nucleation in glasses has recently been questioned (10, 11). Thus, in summary, there appears to be no accurate, quantitative method for assessing glass forming ability available at present.

There have been, however, a number of empirical studies relating to the glass forming ability of a variety of fluoride glass compositions. Moynihan and coworkers (4) have investigated a large number of fluoride glass compositions based upon the ZrF_4, HfF_4 and ThF_4-ZnF_2 systems. They conclude that the optimum composition in the hafnium-barium-lanthanum system is $62HfF_4$ - $33BaF_2$-$5LaF_3$. Also, they find that small additions of AlF_3 tend to stabilize the glasses in this compositional system. In the ThF_4-ZnF_2 based system the $19BaF_2$-$27ZnF_2$-$27YbF_3$-$27ThF_4$ appeared to be the optimum glass forming composition.

A second criteria of a good glass is the existence of a large working range. The typical working range of a fluoride glass is very short. This feature results from the rapid change of viscosity with temperature in fluoride glass melts and the proximity of the temperature at which the glass begins to crystallize (Tx) to the glass transition temperature (Tg). From DSC measurements one may obtain semi-quantitative information regarding $\Delta \equiv Tx-Tg$, which serves as an estimate of the maximum working range of a particular composition. Moynihan et. al (4) and Tran et. al (12) have measured Δ for a variety of fluoride glass compositions. Tran and coworkers also determined the

temperature dependence of the viscosity for these compositions. Ideally, one desires a large value of Δ and a small activation energy for viscous flow (Ea). A ZBLA composition was found to have Δ = 69°C and Ea = 204 kcal/mole. However, a six-component fluoride composition was developed (based upon ZrF_4) with Δ = 103 and Ea = 88 kcal/mole. A ThF_4-ZnF_2 based glass was prepared at RADC with Δ = 140, but viscosity data apparently has not been reported for this glass.

Thus, in summary, it is realized that the choice of glass composition is quite crucial in order to minimize severe processing problems of fluoride fibers. One desires to select good glass formers with a large working range and with little tendency towards phase transformation. To date, such information is available with respect to a moderate number of fluoride compositions. However, our knowledge is inadequate in several respects. First, the data base is incomplete even for those compositions where measurements have been performed. For example, for some compositions Δ is known, but measurements of the temperature dependence of the viscosity have not been performed. Next, in all cases our knowledge of the phase transformation behavior of the fluoride glass compositions is quite scanty. Finally, there does not exist an adequate theoretical framework for predicing the relative glass forming tendencies of these complex compositions.

A second factor which could affect the tendency of the glass to crystallize or phase separate is the raw material purity. For example, in the case of silicate glasses it has been observed that phase separation behavior may be modified by the presence of a fraction of a percent of certain cations such as Al^{+3}. It

has also been noted that the water content of the glass can signficantly affect its phase separation behavior (13, 14). The presence of water in the glass, also, may enhance crystal nucleation and crystal growth rates. James et. al (15) have demonstrated that the nucleation of crystals in $Li_2O \cdot 2SiO_2$ glass is accelerated when the glass possesses an enhanced w[illegible]r content. Wagstaff et. al (16) have investigated the effects of atmospheric [illegible]isture on crystal growth rates in vitreous silica. They observed that at[illegible]heric water enhances the crystal growth rate by 1) acting as a source of o[illegible]n and 2) promoting the formation of hydroxyl groups within the glass. Wagstaff and coworkers concluded that the four factors which had an important bearing on the observed crystallization rates were: 1) the impurity content, 2) the water content in the glass and atmosphere, 3) the state of reduction of the glass, and 4) the surface nucleation characteristics. Also, Abe et. al (17) observed that the surface nucleation of $Ca(PO_3)_2$ glass is promoted by the presence of water in the atmosphere.

The above findings may be of particular importance with regard to the phase transformation behavior of fluoride glasses. The fluoride batch materials are quite hygroscopic and are often present in the starting materials in their hydrated form. Thus, the water incorporated in the raw materials could remain as residual water in the batch and tend to promote crystallization of the fluoride glass. If one employs oxides as the starting materials, then incomplete fluorination of the latter could also produce potential nucleation sites. Trace amounts of residual oxide could precipitate during cooling, providing sites for nucleation of fluoride crystalline material.

Thus, it is suspected that water and impurity metal oxides may be prime factors which abet crystallization. However, experimental investigations have not been performed which verify these suppositions.

Several aspects of the glass melting procedure could strongly influence the phase transformation properties of the glass. For example, the nature of the gas atmosphere employed during melting is believed to be quite significant. It has been suggested (18, 19) that a reactive atmosphere (Cl_2 or CCl_4) over the melt is required to prepare high quality glass, and to prevent the formation of black specks in the bulk of the glass. These black particles are believed to result from a reduction of Zr^{+4} to Zr^{+2}, and it has been argued that their formation will be prevented only by the use of a non-reducing atmosphere. On the other hand, it has been observed that pristine fluoride glass may be prepared in a nitrogen atmosphere if ultrapure starting materials are employed for glassmaking (20). The question of the formation of black particles in the fluoride glass is quite germane to the crystallization problem since such particles will likely serve as effective crystal nucleation sites.

The thermal history of melting, also will be of significance. If the melt is heated for too long a time at the maximum temperature, then there is a good chance that significant amounts of ZrF_4 will be lost due to volatization. In addition, it has been observed that ZrF_4 vapor may condense on the melt at lower temperatures as small crystallites (4). The latter would be effective sites for crystallization of the glass. On the other hand, if the melt is not heated for a long enough period of time at a temperature in excess of the liquidus

temperature, then small fluoride crystallites may persist in the melt. Upon cooling of the melt below the liquidus, these crystallites will provide sites for heterogeneous crystal nucleation.

If a preform method of fiber preparation is used, then several aspects of the preform formation procedure may influence the glass homogeneity. Since the probability of crystallite formation will decrease as the rate of cooling of glass through the maximum crystallization region increases, the precise thermal history experienced by all sections of the preform will be critical. Furthermore, since thicker preforms will cool slowly, such preforms will be more prone to exhibiting devitrification. A second important factor regarding preform preparation is the environment in which the preform is prepared. If the preform is not formed in a controlled atmosphere (inert or reactive; cast in glovebox), the sample will acquire surface water which could promote surface crystal nucleation.

Therefore, there are three major factors which will control the prevention of microphase inclusions in the preform; the choice of glass composition, the thermal history, and the control of impurities. Glasses should be selected well within the glass forming region to avoid crystallization. Thermal schedules should be chosen so that complete melting is produced, but volatization losses are minimized. Also, rapid cooling rates are desirable. Finally, it is important to insure that the glass is free of impurities such as water, metal oxides and other contaminants.

Many of the conditions required for the production of defect-free fluoride fibers are identical to the ones mentioned above for preform preparation. For example, careful control of the atmosphere is required during the fiber pulling operation. However, for fiber pulling the thermal history requirements are more critical. As a result of the short working range of the fluoride compositions there is a good possibility that the glass which is remelted in the fiber pulling furnace will reside for significant periods of time close to the crystallization temperature. Thus, in general, the problem of glass devitrification is expected to be more severe for the fiber pulling operation than for the process of preform fabrication.

Thus, the joint circumstances of short working range and tendency towards devitrification in fluoride glasses causes a complex coupled problem in pulling fibers. On the one hand, constraints as to the maximum and minimum drawing temperature are imposed by the requirement of obtaining a uniform, well controlled fiber diameter. On the other hand, avoidance of certain temperature regimes are desired to minimize the problem of fiber devitrification.

In summary, we have analyzed the ground-based processing steps which are used to produce fluoride fibers, and we have indicated the crucial conditions during processing which may lead to property degradation due to crystallite formation or phase separation.

III. Potential Advantages of Space Processing of Fluoride Fibers

Here we consider the potential advantages of the space processing of fluoride fibers. The potential advantages offered by space will be dependent upon the mode of fiber preparation and the "state of the art" of ground-based fluoride fiber production. For example, if a chemical vapor deposition process is developed for the production of fluoride fiber preforms, then the problems associated with preform fabrication will be overcome. Nevertheless, even if such a process is developed, fiber drawing difficulties may still exist. Under these circumstances one may consider the benefits of drawing fiber in space from a preform prepared on earth.

Currently, preform methods of preparing fluoride fibers appear to be far superior to double crucible draw techniques. Drawing upon our experience with silica fibers, we may anticipate that this situation will persist. Thus, we primarily address preform methods of fiber production.

Three schemes may be envisioned: 1) Preform prepared in space and fiber drawn on earth, 2) preform prepared on earth and fiber drawn in space, or 3) preform prepared and fiber drawn in space. In order to assess whether any of the above are viable options the relative advantages and disadvantages of space and ground-based processing must be evaluated. In this section, only the potential advantages of the space processing of fluoride fibers will be considered.

The major problems associated with preform fabrication are transition metal and/or rare earth ion impurities, water inclusion, and crystallite formation. Since the transition metal (or rare earth) ion impurities are most likely present in the raw materials, space processing will not impact this problem. Also, space offers no particular advantage for water removal. However, the space processing of preforms could affect the tendency for devitrification of preforms. In the microgravity environment of space shuttle, glasses may be formed without the use of a container. This has two potential benefits. First, impurities which might be introduced into the glass from the container during melting would be avoided. Such impurity contamination at a level of even 1 ppb would be detrimental to the optical performance of the fiber at transmission loss levels below 1 db/km. Next, it is possible that the tendency towards preform devitrification may be suppressed. The basis for the latter conjecture is as follows. The vast majority of glasses are found to crystallize heterogeneously. It is well known that foreign bodies which contact the glassmelt may lower the required free energy to form a glass-crystal interface. Thus, crystallites will tend to form preferentially on the surface of such bodies. The crucible which contains the melt could supply impurity particles to the melt which in turn abets crystallite formation. Similarly the mold into which the glassmelt is poured could provide effective heterogeneous nucleation sites. However, in space the glass could be prepared and the preform fabricated in a containerless fashion. In this manner heterogeneous nucleation of crystallites in the preform could be avoided. It appears as though this feature is the main advantage of preparing preforms in space.

Next we consider the potential advantages of drawing fiber in space. There are two general experimental schemes by which this procedure may be executed.

The fiber may be drawn aboard the space vehicle using the usual ground-based fiber drawing apparatus, or the fiber may be drawn in space (outside of vehicle). If the former option is chosen, then the only difference between ground-based and space production of fibers will be related to the fluid dynamics of the fiber pulling operation. It may be desirable to draw fibers at relatively high temperatures in a regime where the material is somewhat fluid (see Section IV for more complete discussion of this point). However, it is known from experience (i.e., drawing of silicate fibers) that on earth it is impossible to draw fibers at low viscosities since diameter control is lost under these conditions. Under microgravity conditions, however, the flow conditions will be altered, and the possibilities for low viscosity drawing will be considered in the next section.

If, on the other hand, fibers are drawn exterior to the vehicle two new additional features come into play. First, the radiative component of the fiber cooling rate will be larger because of the nearly 0°K background temperature. Rapid cooling rates are desirable in order to avoid devitrification. Also, the high vacuum condition makes possible the avoidance of fiber contamination during the drawing process. In addition, extremely long lengths of fiber may be readily drawn.

Thus, a number of attractive features appear for preform fabrication and/or fiber drawing in space. However, as will be discussed subsequently, many severe difficulties are encountered, also, in attempting to produce fibers in space. In addition, some of the apparent advantages of space processing which were mentioned above appear to be of marginal utility.

IV. Evaluation of the Advantages and Problems Associated with Fluoride Glass Fiber Production in Space

In Section III some of the potential benefits which could be derived from the space processing of fluoride glass fibers were mentioned. In this Section these possible advantages will be discussed in further detail. Also, the unique problems associated with the production of fluoride glass fibers in space will be considered.

Of utmost importance is the consideration of gravitational effects on the fluid dynamics of drawing fluoride optical fibers. In general, fiber drawing is a very complex process, and the complete set of equations governing this process consists of a set of complicated coupled nonlinear partial differential equations for fluid flow and heat transfer. In order to simplify the analysis of the fiber drawing process, the fiber may be divided into three regions (21) [see Figure 1.] In the first region, termed the forming zone, the fiber diameter changes rapidly and the characteristics of the flow may be quite sensitive to the procedure used for the heating of the glass. The second region, called the draw-down zone, is characterized by small velocity gradients in the radial direction and significant material acceleration in the axial direction. In the third zone it is assumed that the material is essentially a solid. "Most fiber stability studies place major emphasis on the draw-down region, because of its physical importance and mathematical tractability" (22). For our consideration of the effects of gravity on the glass flow behavior we, too, solely consider this region. However, as we will discuss subsequently,

consideration of Region 3 is of paramount importance when we compare the pulling force in microgravity and earth-based fiber pulling operations.

In this preliminary analysis we ignore the thermal problem and analyze the isothermal steady-state flows following the procedure of Matovich and Pearson (21) and Geyling (22). This procedure, albeit crude, should provide an indication of the importance of gravity in determining the nature of the steady-state flows. The relevant governing equations for the draw-down region are (21, 22):

$$\frac{\partial V}{\partial x} + \frac{1}{r}\frac{\partial}{\partial r}(ru) = 0 \tag{1}$$

$$\rho\left(u\frac{\partial u}{\partial r} + V\frac{\partial u}{\partial x}\right) = \frac{1}{r}\frac{\partial}{\partial r}(r\tau_{rr}) - \frac{\tau_{\theta\theta}}{r} + \frac{\partial \tau_{rx}}{\partial x} \tag{2}$$

$$\rho\left(u\frac{\partial V}{\partial r} + V\frac{\partial V}{\partial x}\right) = \rho g + \frac{1}{r}\frac{\partial}{\partial r}(r\tau_{rr}) + \frac{\partial \tau_{xx}}{\partial x} \tag{3}$$

It is assumed here that glass is a Newtonian liquid and the flow is axisymmetrical. In Eqs. (1-3) x and r are the axial and radial coordinates respectively, V and u are the axial and radial components of the velocity respectively, ρ is the density, g is the gravitational constant, and τ_{ij} is the i,j components of the stress tensor. The stress tensor components for an incompressible fluid for the present case are given by:

$$\tau_{rr} = -p + 2\eta \frac{\partial V}{\partial r} \tag{4a}$$

$$\tau_{rx} = \eta \left(\frac{\partial u}{\partial r} + \frac{\partial V}{\partial x} \right) \tag{4b}$$

$$\tau_{\theta\theta} = -p + \frac{2\eta V}{r} \tag{4c}$$

$$\tau_{xx} = -p + 2\eta \frac{\partial u}{\partial x} \tag{4d}$$

where p is the pressure and η is the shear viscosity. The following boundary conditions are imposed at x = 0,

$$a(x=0) = a_0 \tag{5a}$$

$$V(x=0) = V_0 \tag{5b}$$

$$u(x=0) = u_0 \tag{5c}$$

where a is the fiber radius. The additional boundary conditions must be satisfied too (see Figure 1).

$$V(r, x=L) = V_L \tag{6}$$

$$V = u \frac{\partial a}{\partial x} \tag{7}$$

It is apparent that even the isothermal, steady-state governing equations are enormously complex. An approximation scheme has been developed by Matovich and Pearson for the draw-down region based on the observation that the change in fiber radius is quite small in this region. This scheme results in a perturbation expansion related to the smallness of the rate of change of a. The zero order equation for V (in dimensionless form) in this scheme is shown in Eq. (8) [see Appendix A].

$$\psi \psi'' - (\psi')^2 = Re\, \psi^2 \psi' - \left(\frac{Re}{Fr}\right)\psi + \left(\frac{Re}{We}\right)\sqrt{\psi}\, \psi' \tag{8}$$

In Eq. (8) Re, Fr, We, are the Reynolds, Froude and Weber numbers, respectively, and they are given by,

$$Re = \frac{\rho L V_L}{3\eta} \tag{9a}$$

$$Fr = \frac{V_L^2}{gL} \tag{9b}$$

$$We = \frac{2a V_L^2 \rho}{\sigma} \tag{9c}$$

In Eq. (9c) σ is the surface tension. In Eq. (8), ψ is defined by

$$\psi(y) = \frac{V(x/L)}{V_L} \tag{10}$$

One notes that the zero order reduced axial velocity is solely a function of the reduced axial coordinate, y, and the primes in Eq. (8) refer to differentiation with respect to this variable. Eq. (8) must satisfy the following boundary conditions.

$$\psi(y=0) = 1 \tag{11a}$$

$$\psi(y=1) = E \equiv V_L/V_0 \tag{11b}$$

Eq. (8) may be simplified by introducing a new variable $\Phi \equiv \psi^{1/2}$. Then after a bit of manipulation we obtain

$$\frac{d}{dy}\left\{\frac{\Phi'}{\Phi} - \frac{Re}{2}\Phi^2 + \frac{Re}{We}\Phi^{-1}\right\} = -\frac{1}{2}\frac{Re}{Fr}\Phi^{-2} \tag{12}$$

For ground-based processing conditions a solution of the above equation is required in its complete form. However, under microgravity conditions the righthand side of Eq. (12) is quite small, and we may write

$$\frac{d}{dy}\left\{\frac{\Phi'}{\Phi} - \frac{Re}{2}\Phi^2 + \frac{Re}{We}\Phi^{-1}\right\} = 0 \qquad (12')$$

The above equation may be integrated to yield

$$\frac{d\Phi}{dy} = \frac{Re}{2}\Phi^3 - \frac{Re}{We} + C\Phi \qquad (13)$$

Eq. (13) may be integrated directly to obtain

$$\frac{Re}{2}y + D = A_1 \ln\left[\frac{(\Phi - \Phi_1)}{(\Phi^2 + \Phi\Phi_1 - a_1'/\Phi_1)^{1/2}}\right] - \frac{3A_1\Phi_1}{\xi^{1/2}}\tan^{-1}\left\{\frac{2\Phi + \Phi_1}{\xi^{1/2}}\right\} \qquad (14a)$$

with

$$\xi = -\Phi_1^2 - \frac{4a_1'}{\Phi_1} \qquad (14b)$$

$$A_1 = \left(2\Phi_1^2 - a_1'/\Phi_1\right)^{-1} \qquad (14c)$$

$$a_1' = -(Re/We)/(Re/2) \qquad (14d)$$

and Φ_1 is the real root of

$\frac{Re}{2}\Phi^3 + C\Phi - \frac{Re}{We} = 0$, when two complex roots occur. D, in Eq. (14a) is an integration constant. When the latter equation possesses three real roots, then the solution to Eq. (13) is given as

$$\frac{Re}{2} y + D' = \frac{1}{DET} \ln \left\{ \frac{(\bar{\Phi} + |\bar{\Phi}_3|)^{(\bar{\Phi}_1 + |\bar{\Phi}_2|)}}{(\bar{\Phi} + |\bar{\Phi}_2|)^{(\bar{\Phi}_1 + |\bar{\Phi}_3|)} (\bar{\Phi} - \bar{\Phi}_1)^{(|\bar{\Phi}_2| - |\bar{\Phi}_3|)}} \right\} \quad (15a)$$

where Φ_1 is the positive root, and Φ_2, Φ_3 are the negative roots of $\frac{Re}{2}\Phi^3 + C\Phi - \frac{Re}{We} = 0$, and DET is given by

$$DET \equiv \begin{vmatrix} 1 & 1 & 1 \\ (\bar{\Phi}_2 + \bar{\Phi}_3) & (\bar{\Phi}_1 + \bar{\Phi}_3) & (\bar{\Phi}_1 + \bar{\Phi}_2) \\ \bar{\Phi}_2 \bar{\Phi}_3 & \bar{\Phi}_1 \bar{\Phi}_3 & \bar{\Phi}_1 \bar{\Phi}_2 \end{vmatrix} \quad (15b)$$

The constants D, D' and C appearing in Eqs. (14a, (15a) and (13) may be obtained readily from the boundary conditions.

An analytical solution for Eq. (12) could not be found, and hence Eq. (12) was integrated numerically using a Runge-Kutta method.

From an inspection of the governing equation it is apparent that the steady state velocity will be governed by the choice of four dimensionless parameters; Re, Re/We, Re/Fr, and E. In a crude sense Re is a measure of viscous effects, Re/We a measure of surface tension effects, Re/Fr a measure of gravitational effects, and E is that ratio of velocities at the beginning and end of the draw-down zone and will be related to the pulling conditions in a complex manner.

Φ was computed as a function of the reduced axial distance, y, for several sets of the dimensionless groups appropriate for fluoride glass fiber pulling. The results are displayed in Figures (2-4). Several comments are warranted regarding these plots. First it is observed that in all cases Φ increases without limit for finite y (and $y \leq 1$). This behavior is not physically realistic and it stems from our neglect of the cooling process. If fiber cooling were accounted for, then (in a crude sense) the Reynolds number decreases for larger y and Φ is well behaved (see discussion below). These graphs also indicate that no solution exists for Φ where ψ satisfies boundary condition Eq. (11b). Thus, in order to generate these curves a condition on the initial derivative of Φ was used in place of Eq. (11b). Next, we note that for smaller values of these dimensionless groups the increase in velocity is slower and the abrupt rise in velocity occurs at larger axial distances. This feature supports the observation made above that accounting for fiber cooling will

remove the rapid increase in velocity since cooling causes an increase in viscosity and thus a decrease in the magnitudes of the dimensionless groups. Finally, and of most signficance for this study, we observe that the effect of gravity on the velocity profile is quite small (compare curves with Fr/Re = 0 and Fr/Re ≠ 0). For the dimensionless parameters chosen for Figure 4, the difference in velocity profile for Fr/Re = .2 and Fr/Re = 0 was so small that the two sets of points essentially lie on the single curve which was drawn.

In order to obtain a more realistic form for the velocity profile, yet avoid the complex couple fluid mechanical-thermal problem, we have accounted for the increase in viscosity as a result of cooling in the following simple manner. Paek and Kurkjian (23) have obtained the following expression for the temperature of a fiber during drawing,

$$\theta = \exp\left\{\frac{-\beta x}{aV}\right\} \tag{16a}$$

with

$$\theta \equiv (T - T_0)/(T_i - T_0) \tag{16b}$$

$$\beta \equiv \frac{4h}{\rho C_p} \tag{16c}$$

In Eqs. (16a-c) T_0 is the ambient temperature, T_i is the temperature at x = 0, C_p is the constant pressure specific heat and h is the heat transfer coefficient. The temperature dependence of the viscosity has been shown to exhibit Arrhenius behavior so that the viscosity, η, may be expressed as

$$\ln \eta = A_1 + \frac{A_2}{T_0 + (T_i - T_0) \exp\left\{ \frac{-\beta x a}{a^2 V} \right\}} \tag{17a}$$

Since, by the condition of mass conservation

$$a^2 V = \text{constant} \tag{18a}$$

$$a^2 V = a_0^2 V_0 \tag{18b}$$

then we have

$$\ln \eta = A_1 + \frac{A_2}{T_0 + (T_i - T_0) \exp\left\{ \frac{-\beta x a}{a_0^2 V_0} \right\}} \tag{17b}$$

However, for the one dimensional analysis for fluid flow to be valid we require $\partial a/\partial x \ll 1$. Thus, we may treat a as approximately constant in Eq. (18b) and obtain η solely as a function of x (see Figure 5). With the following choice of parameters: $A_1 = -71.2$, $A_2 = 4.4288 \times 10^4$ deg K, $\beta = .0224$ cm/sec, $a_0 = 10^{-2}$ cm, $V_0 = 10$ cm/sec, $T_0 = 300$ deg K, and $T_i = 622$ deg K, we used

Eq. (18b) in Eq. (12) to recompute Φ. The results are displayed in Figure (6). The curve denoted by η = constant was reproduced from Figure (2), and shows the rapid increase in Φ for the isothermal calculation. On the other hand, one observes from this figure that a smooth well behaved velocity profile is obtained when fiber cooling is taken into account. It is important to note, however, that the calculation described above will become unrealistic when the viscosity becomes excessively great since then the constituitive equations (Eqs. 4a-4d) will be invalid.

A quantity of prime importance is the drawing force which is exerted on the fiber. The drawing force consists of several terms. First, the drawing force in a microgravity environment is given by (22)

$$F = \frac{2\pi a \sigma}{\left(1+\left[\frac{\partial a}{\partial x}\right]^2\right)^{1/2}} + 2\pi \int_0^a r \tau_{xx}\, dr \qquad (19)$$

On earth we must also consider the gravitational force. The gravitational force on a small volume element, dV, is $\rho g\, dV$. We separate the gravitational force into two parts; that exerted on Region 2 and that exerted on Region 3 (Region 1 will be neglected). The total gravitational force in Region 2, F_{g2} is given by

$$F_{g2} = -\int_0^L dx\, 2\pi \rho g \int_0^{a(x)} r\, dr = -\pi \rho g \int_0^L a^2(x)\, dx \qquad (20)$$

Using Eq. (18b) in Eq. (20) we find

$$F_{g2} = -\pi \rho g a_o^2 V_o \int_0^L \frac{dx}{V(x)} \tag{21}$$

The gravitational force on the solid portion of the fiber, F_{g3}, is given by

$$F_{g3} = -\pi a_f^2 \rho g L' \tag{22}$$

where in Eq. (22) $a_f = a(x = L)$ and L' is the length of the solid portion of the fiber. Eq. (17) may be simplified by recognizing that $1 \gg \partial a/\partial x$. Hence, the total pulling force may be found from Eqs. (17), (21) and (22).

$$F = 2\pi a_f \sigma + 2\pi \int_0^{a_f} r \tau_{xx} \, dr - \pi \rho g a_o^2 V_o \int_0^L \frac{dx}{V(x)} - \pi a_f^2 \rho g L' \tag{23}$$

In order to evaluate the pulling force we need to know the constituitive equation over the entire length of Region 2. However, since the viscoelastic behavior of the fluoride glasses have not been studied, we approximate τ_{xx} by its purely viscous behavior and truncate the size of Region 2. Thus, if Eq. (4d) is employed in conjunction with Eq. (23) we find

$$F = \pi a_f \sigma + 3\eta \pi a_f^2 \left(\frac{\partial V}{\partial x}\right)_{L^*} - \pi \rho g a_o^2 V_o \int_0^{L^*} \frac{dx}{V(x)} - \pi a_f^2 \rho g \left[L' + (L - L^*)\right] \tag{24}$$

Introducing the dimensionless velocity and distance into Eq. (24) a dimensionless pulling force, $\bar{F}$ may be found:

$$\bar{F} \equiv \frac{F}{(3\pi\eta V_0 a_f^2/L^*)} = \frac{L^*\sigma}{3a_f\eta V_f}\left(\frac{V_f}{V_0}\right) + \left(\frac{\partial\psi}{\partial y}\right)_{y=1} - \frac{\rho g (L^*)^2}{3\eta V_f}\left(\frac{V_f}{V_0}\right)\left(\frac{a_0}{a_f}\right)^2 \int_0^1 \frac{dy}{\psi}$$

$$- \frac{\rho g (L^*)^2}{3\eta V_f}\left(\frac{V_f}{V_0}\right)\left(\frac{L'}{L^*}\right) \qquad (25)$$

$$= 2E\frac{Re^*}{We^*} + \left(\frac{\partial\psi}{\partial y}\right)_{y=1} - E^2\frac{Re^*}{Fr^*}\int_0^1 \frac{dy}{\psi} - \frac{Re^*}{Fr^*} E\frac{L'}{L}$$

In obtaining Eq. (25) we have employed Eq. (18b) and have assumed that $L' >> L - L^*$. The * on the dimensionless groups indicates that they are to be taken at $X = L^*$ (i.e., $y = 1$). The first two terms for the pulling force are positive and are related to surface tension and viscous forces, respectively. The second two terms are negative and are related to gravitational forces in Region 2 and Region 3, respectively (with the provisos mentioned above). For the conditions chosen for the previous computations of the velocity field, it is easy to show that $\left(\frac{\partial\psi}{\partial y}\right)_{y=1} >> 2E\left(\frac{Re^*}{We^*}\right)$. Also, for typical fiber pulling conditions we expect that $\frac{L'}{L^*} >> E\int_0^1 \frac{dy}{\psi}$. Therefore, to a good approximation

$$\bar{F} \approx \left(\frac{\partial\psi}{\partial y}\right)_{y=1} - \frac{Re^*}{Fr^*} E\frac{L'}{L} \qquad (26)$$

Within the framework of the one-dimensional model, and without accounting for viscoelastic effects, it is not possible to make reliable estimates for $\overline{F}$. $\partial\psi/\partial y$ may be approximted fairly well since it is found to be slowly varying, but Re^*/F_r^* is a rapidly decreasing function of distance and thus cannot be estimated accurately. In any case, the important point to note is that the pulling force consists solely of positive terms in a microgravity situation while on earth positive and negative terms appear. Thus, for example, if $L' >> L$ it is possible that $\overline{F}$ may be negative. This would indicate that for the specified pulling conditions, fiber could not be drawn on earth, but possibly could be drawn in space. In order to confirm that fiber could be produced under such conditions it would be necessary to perform a stability analysis on the steady-state base flow.

Hence, we have reached the following conclusions regarding the effect of gravity on the fiber pulling process. Gravity plays a very small role in determining the steady-state fluid flows for typical values of the dimensionless groups appropriate for fluoride glass fiber pulling. Furthermore, for those cases where gravity plays a perceptible role in determining the steady-state flows, it tends to stabilize these flows in the sense that the velocity increases more slowly as a function of axial position. On the other hand, gravity may play an important role in the determination of the fiber pulling force. In a zero g environment there is no restriction on the steady-state flows since the pulling force is always positive. On earth, however, there are conditions where a negative pulling force obtains. Such flows are unobtainable and indicate an

instability. Thus, there exists a class of steady-state flows which are unobtainable on earth, but are permitted in space. In order to ascertain if such flows are stable, however, a stability analysis must be performed.

A second factor of importance is the cooling rate of the fiber. Here, an approximate analysis shows that the cooling rate of a fiber drawn into free space will be smaller than that drawn in a conventional atmosphere. The analysis begins with the heat transfer equation shown below.

$$\rho C_p \frac{\partial T}{\partial t} + \rho C_p V_x \frac{\partial T}{\partial x} =$$

$$\frac{1}{r}\frac{\partial}{\partial r}\left([k + k_R(T)] r \frac{\partial T}{\partial r}\right) + \frac{\partial}{\partial x}\left([k + k_R(T)] \frac{\partial T}{\partial x}\right) \quad (27)$$

In Eq. (27) ρ is the glass density, C_p is the constant pressure specific heat of the glass, T is the glass temperature, r and x are the radial and axial coordinates, respectively, V_x is the x component of the velocity, k and k_R are the ordinary and radiative heat conductivity coefficients, and t is the time. If $Pe \equiv V_x a \rho C_p / k \gg 1$, then the last term on the right side of Eq. (27) may be neglected (a is the fiber diameter). Here, we find $Pe \sim 100$, and thus Eq. (27) reduces to

$$\rho C_p \frac{\partial T}{\partial t} + \rho C_p V_x \frac{\partial T}{\partial x} = \frac{1}{r}\frac{\partial}{\partial r}\left[(k + k_R(T)) r \frac{\partial T}{\partial r}\right] \quad (28)$$

If we multiply Eq. (28) by rdr and integrate from 0 to a we obtain

$$I \equiv \int_0^a r dr \left\{ \rho c_p \frac{\partial T}{\partial t} + \rho c_p V_x \frac{\partial T}{\partial x} \right\} = \left[k + k_R(T) \right] a \left(\frac{\partial T}{\partial r} \right)_{r=a} \tag{29}$$

However, the right side of Eq. (29) is the heat flux from the outer surface of the fiber, and consequently may be written as follows:

$$I = -a \left\{ h (T_a - T_\infty) + \sigma \varepsilon (T_a^4 - T_\infty^4) \right\} \tag{30}$$

In Eq. (30) h is the heat transfer coefficient, Ta is the temperature at the fiber surface, T_∞ is the ambient temperature far from the fiber, ε is the emissivity, and σ is the Stephen-Boltzmann constant. Also, if

$$\bar{T} \equiv \int_0^a r dr\, T \tag{31}$$

$$\rho c_p \left[\frac{\partial \bar{T}}{\partial t} + V_x \frac{\partial \bar{T}}{\partial x} \right] = -a \left\{ h (T_a - T_\infty) + \sigma \varepsilon (T_a^4 - T_\infty^4) \right\} \tag{32}$$

In deriving Eq. (32) we have once again assumed that V_x is nearly constant in the radial direction. We note that it may be possible to compare the relative effectiveness of cooling the fiber in space and on earth merely by calculating the right side of Eq. (32). We have

$$I_{space} = \varepsilon \sigma T^4 \tag{33a}$$

$$I_{earth} = h(T - T_\infty) + \sigma\varepsilon(T^4 - T_\infty^4) \tag{33b}$$

Hence,

$$I_{earth}/I_{space} = \frac{h(T-T_\infty)}{\varepsilon \sigma T^4} + 1 - \left(\frac{T_\infty}{T}\right)^4 \tag{34}$$

Even if we choose values of ε and T favorable for rapid cooling in space (T = 800°K and ε = 1) and assume $T_\infty \approx 300$°K we find that $I_{earth}/I_{space} \approx 6.7$. Therefore, radiative cooling is rather unimportant and the fiber will cool more rapidly by convective heat transfer.

V. Required Ground-Based Experimentation

We have observed that a potential advantage of drawing fibers in space hinges upon the possibility of utilizing temperature regions inaccessible to fiber pulling in a ground-based environment. However, in order to exploit this possibility one must ascertain that the crystallization rates are not too large in this temperature region. Thus, the main focus of the experiments should entail a detailed investigation of the high temperature crystallization behavior of a prototype heavy metal fluoride glass composition. This would include studying both nucleation behavior and kinetics and crystallite growth rates and behavior.

The experimental program would consist of several tasks. First, a study of the isothermal crystallization behavior of a fluoride glass would be performed. This would entail studying crystal development occurring internally in the glass as well as the surface crystallization behavior.

Two methods may be employed to study the isothermal crystallization of the glass. In one method the glass melt is cooled to room temperature, and glass samples are subsequently heated to those temperatures at which the crystallization studies are to be performed. In a second method the melt (or a portion of the glassmelt) may be cooled directly to the desired temperature(s) at which the crystallization behavior may be studied. Both methods should be employed and the resulting crystallization behavior compared.

Since the details of the glass preparation procedure could strongly influence the crystallization behavior of fluoride glass, the crystallization behavior must be studied as a function of preparation procedure. Once this data has been obtained, then the preparation procedure may be varied in order to minimize crystallization at high temperatures. In order to accomplish the latter the following factors will be considered.

It has been observed that the purity of the raw materials could influence glass forming ability in typical fluoride glass compositions. Thus, glasses should be prepared using both high purity and ultra-high purity starting materials and comparisons should be made of the crystallization behavior of the corresponding glasses.

The crystallization behavior of these glasses may be quite sensitive to the oxygen and/or water content in the melt. Furthermore, it has been observed that the crystalline starting materials can be present in hydrated forms. Thus, an investigation of the effects of preheat-treatment of the raw materials prior to glassmaking and varying $NH_4F \cdot HF$ concentrations should be made. Since these procedures will alter the water and oxide content of the melt, such techniques will help establish the sensitivity of crystallite formation to oxide and water impurity content. In addition, chemabsorption of water from the air on the glass surface could affect the nature of surface crystallization, and this should also be studied.

Prior to the heat treatment of the glasses, a variety of analyses may be performed to characterize the glass condition. The glass compositions may be verified by atomic absorption techniques. Wet chemistry methods of chemical analysis and X-ray fluorescence procedures may be developed for analysis too. IR spectroscopy may be employed to ascertain the water content of the glasses.

Heat treatments may be performed in tubular furnaces with temperature accuracy of no worse than ±1°C in the hot zone. The samples may be contained in vitreous carbon or platinum boats. Heat treatments may be performed in air, dry N_2 (or other inert atmosphere) and reactive atmosphere. Samples should be heated at several temperatures for prescribed time sequences.

Powder X-ray diffraction may be used for the analysis of the crystallized glass. Also, microprobe and EDAX may be utilized in conjunction with XRD to obtain information regarding the chemical nature of any unknown crystalline phases. In addition, SEM and optical microscopy may be employed to study the crystal morphology and to seek for any signs of internal crystallite formation.

The studies described above would provide information as to the crystallization behavior of fluoride compositions which have been isothermally heated at high temperatures. If the results of such studies appear encouraging, then similar studies should be performed on fibers.

Finally, a study to detect the possible development of amorphous phase separation in compositions of interest might be in order. REM and SAXS could be

used for detection of phase separation occurring on a submicroscopic scale in heat-treated glasses. To date, there has been no report of experimental detection of possible amorphous phase separation in any fluoride glass composition that has been prepared. However, the possibility that metastable amorphous phase separation may occur in ZrF_4-BaF_2-based compositions is suggested by thermodynamic computer calculations that have been carried out on this binary system (24). In particular, in silicate and borate binary glass systems that possess s-shaped liquidus curves, metastable amorphous immiscibility is commonly found to occur below the inflection points at lower temperatures (25). The aforementioned calculations (24) predict the occurrence of such an S-shaped liquidus on the BaF_2-rich side of the binary. If this is also indicative that metastable immiscibility occurs in this composition range, then there is also the possibility that such phase separation may occur on the ZrF_4-rich side of the immiscibility dome if the liquidus curve lies near Tg in the glass formation region of the phase diagram.

If experimental evidence is obtained that amorphous phase separation does occur, then a study of the effect of the concentration of minor constituents in the glass on the shape and critical temperature of the immiscibility dome should be performed. It is well known, for instance, that in silicate and borosilicate glasses which exhibit metastable phase separation, the addition of trace amounts of Al cation has dramatic effects on lowering the immiscibility curve, which hence, effectively decreases the tendency toward phase separation.

VI. Required Computations and Modelling

It will be necessary to know the thermal history of the glass during the fiber drawing process in order to predict if a schedule can be suggested which avoids fiber devitrification. The experimentally obtained isothermal crystallization data then may be used in conjunction with the specified thermal history to predict the extent of devitrification for a given thermal schedule.

The thermal history of the glass may be roughly divided into several regimes: 1) $T>Te$, 2) $Te>T>T_D$ and 3) $T_D>T$ where Te is the liquidus temperature and T_D is the fiber drawing temperature. In Region 1 the thermal history is irrelevant since crystallite formation cannot occur above Te. However, it is important that the glassmelt be raised to a sufficiently high temperature (in Region 1) so that all remnant crystallites are dissolved, but not so high as to cause a compositional variation due to excess vaporization of a volatile component. The thermal history in Region 2 will be dependent upon the details of the experimental scheme employed for fiber drawing. For example, the glass melt may be held at T^*, where $T^*>Te$ and periodically a small portion of the melt may be rapidly cooled to T_D and then held isothermally at T_D. The time a small volume element of glass spends at T_D will depend upon the total volume of glass held at T_D and the fiber drawing speed. However, this portion of the thermal history profile may be easily computed. The third portion of the thermal history of the glass will depend upon the cooling rate of the fluoride glass fiber. Since during fiber drawing operation the glass simultaneously flows and cools, the temperature equation is coupled to the fluid flow

equation. This system of partial differential equations is quite complex. However, approximations may be made which decouple these equations and which allow one to treat the thermal problem independently. The thermal conductivity data which will be required for these calculations may be obtained from measurements. Heat transfer coefficients could be estimated from experimental data.

The experimentally obtained fiber crystallization data could then be used in conjunction with the fiber cooling calculations to predict the extent of devitrification as a function of fiber drawing procedure.

We have shown that certain flows are possible in a microgravity environment which are not obtainable on earth. However, our analysis was based upon a steady-state flow analysis. In order to demonstrate that these flows are stable in space a stability analysis must be performed.

There are three different mechanisms which can cause instability, and in general these mechanisms are coupled.

1. The first mechanism is caused by surface tension which tends to accumulate fluid into periodic "beads". If viscous stresses are overcome then ultimately individual droplets may "pinch off" (Rayleigh instability). This type of instability is more likely to occur in the low viscosity regime where surface tension effects are of greater relative importance.

2. The second mechanism is triggered by a tensile stress concentration which reduces the cross-sectional area and results in a single, "run-away" tensile separation. Here, surface tension and viscous effects tend to stabilize the process. This type of instability may be important in the cold parts of fibers where the effect of surface tension is negligible. Both of these instabilities are associated with the shape of the outer surface of the fiber and do not destroy its axial symmetry.

3. The third type of instability is caused by local compression which leads to an axial instability, i.e., buckling of the fiber.

All of these instability mechanisms are "contained" in the mathematical model derived in this work. However, their analysis is difficult as a result of the nonlinear nature of the partial differential equations. Since, from the practical viewpoint, only the demonstration of stability (or instability) is essential (while the post-instability behavior is not so important), linearization of the governing equations with respect to a selected stationary regime and application of the perturbation technique is the most promising mathematical tool for the stability analysis. The complexity of the problem will depend upon the degree of simplificaiton which can be made for the governing equations for the selected stationary regime. If the technique of variable separation for the linearized model is not applicable, then the partial differential equations will have to be converted to finite difference equations and numerical methods will be required for solution.

VII. Summary

The ground-based processing sequences used to produce fluoride fibers have been analyzed and those steps which could lead to fiber property degradation as a result of phase separation or crystallite formation have been identified. It was observed that in general three major factors control the prevention of microphase inclusions in the preform; the choice of the glass composition, the thermal history, and the control of impurities. Containerless processing of preforms could play some role in alleviating crystallite formation by avoiding the contact of the melt with a container. The above factors are also of importance for the production of defect-free fibers. However, as a result of the short working range of most fluoride glass compositions and the requirement of maintaining stable fluid flows during fiber pulling operations, the difficulty of producing microinclusion-free fibers will be greater than that of preparing defect-free preforms.

Our preliminary analysis of the fiber pulling process has led to the following conclusions. For the values of the physical parameters pertinent to fluoride glass fibers, gravity plays a very small role in determining the characteristics of the fluid flow. However, at higher temperatures where the viscosity is low, gravitational effects could be quite important in determining the pulling force on the fiber. In particular, we have estimated that under certain conditions fiber pulling would be impossible on earth since a negative pulling force is predicted. Therefore, low gravity space processing of fluoride fibers would be advantageous only if it is possible to pull fibers at relatively high

temperatures. Our estimates of fiber cooling rates indicate, however, that fibers drawn in space will cool at rates equal to or less than those on earth. Hence, knowledge of the crystallization rates of fluoride glasses at high temperatures will be critical in determining the possible advantages of drawing fluoride fibers in space. If crystallization rates are sufficiently slow, then high temperature drawing of fluoride glass fibers in space could be feasible if the fluid flows are stable.

Appendix A

In this appendix we provide an estimate for the regime of validity of the one-dimensional equation used in Section IV (see Eq. (8).

The equations governing an axisymmetric viscous flow are

$$\rho\left(V\frac{\partial V}{\partial x}+u\frac{\partial V}{\partial r}\right)=-\frac{\partial p}{\partial x}+\eta\left(\frac{\partial^2 V}{\partial r^2}+\frac{1}{r}\frac{\partial V}{\partial r}+\frac{\partial^2 V}{\partial x^2}\right) \tag{A1}$$

$$\rho\left(V\frac{\partial u}{\partial x}+u\frac{\partial u}{\partial r}\right)=-\frac{\partial p}{\partial r}+\eta\left(\frac{\partial^2 u}{\partial r^2}+\frac{1}{r}\frac{\partial u}{\partial r}-\frac{u}{r^2}+\frac{\partial^2 u}{\partial x^2}\right) \tag{A2}$$

$$\frac{\partial(rV)}{\partial x}+\frac{\partial(ru)}{\partial r}=0 \tag{A3}$$

where x and r are the axial and radial coordinates, respectively, and V and u are the axial and radial components of velocity, respectively. In order to obtain an approximate equation for the axial component of velocity, we approximate Eq. (A1) by decoupling it from the remaining equations. From an inspection of Eq. (A1) we note that it is coupled to the other equations only through the term $u\frac{\partial V}{\partial r}$. We may rewrite Eq. (A1) in the following form:

$$V\frac{\partial V}{\partial x} + \left(u - \frac{\nu}{r}\right)\frac{\partial V}{\partial r} = -\frac{1}{\rho}\frac{\partial p}{\partial x} + \nu\left(\frac{\partial^2 V}{\partial r^2} + \frac{\partial^2 V}{\partial x^2}\right) \qquad \text{(A1')}$$

where ν is the kinematic viscosity ($\equiv \eta/\rho$). If

$$\frac{\nu}{r} >> u \qquad \text{(A4)}$$

then the coefficient of $\frac{\partial V}{\partial r}$ may be approximated by $-\frac{\nu}{r}$ and Eq. (A1') is uncoupled. Also, by integrating Eq. (A3) with respect to r, we find that

$$u \approx -\frac{a}{2}\frac{\partial V}{\partial x} \qquad \text{(A5)}$$

In obtaining Eq. (A5) we have assumed that $\frac{\partial V}{\partial x}$ is roughly constant in the radially direction. Thus, the decoupling condition may be written as

$$\frac{2\nu}{a^2} >> \left|\frac{\partial V}{\partial x}\right| \qquad \text{(A6)}$$

Since $a \sim 10^{-2}$ cm. we have

$$2\times 10^{4}\nu >> \left|\frac{\partial V}{\partial x}\right| \qquad \text{(A7)}$$

as the condition for the validity of the approximate one-dimensional velocity equation.

References

1. M. Poulain and J. Lucas, Mat. Res. Bull. 10, 243 (1975).

2. M. G. Drexhage, C. T. Moynihan and M. Saleh-Boulos, Mat. Res. Bull. 15, 213 (1980).

3. T. Miya, Y. Terunuma, T. Hosaka and T. Miyashita, Electron. Lett. 15, 106 (1979).

4. C. T. Moynihan, K. H. Chung, O. L. Gavin, A. J. Bruce, E. O. Gbogi and M. Boulos, Metallic Halide Optical Glasses: Synthesis and Characterization of IR Transmitting Fluoride Glasses, Final Technical Report to Rome Air Development Center (RADC-TR-82-264), October 1982.

5. D. R. Uhlmann, J. Amer. Ceram. Soc. 66, 95 (1983).

6. O. Turnbull, Contemp Phys. 10, 473 (1969).

7. H. Yinnon and D. R. Uhlmann, J. Non-Cryst. Solids 44, 37 (1981).

8. P. I. K. Onorato and D. R. Uhlmann, J. Non-Cryst. Solids 22, 367 (1976).

9. D. R. Uhlmann, J. Non-Cryst. Solids 7, 337 (1972).

10. G. F. Neilson and M. C. Weinberg, J. Non-Cryst. Solids 34, 137 (1979).

11. E. G. Rowlands and P. J. James, Phys. Chem. Glasses 20, 1 (1979).

12. D. C. Tran, R. J. Ginther and G. H. Sigel, Jr., Mater. Res. Bull. 17, 1177 (1982).

13. M. C. Weinberg and G. F. Neilson, J. Mater. Sci. 13, 1206 (1978).

14. N. J. Kreidl and M. S. Maklad, J. Amer. Ceram. Soc. 52, 508 (1969).

15. C. J. R. Gonzalez-Oliver, P. S. Johnson and P. F. James, J. Mater. Sci. 14, 1159 (1979).

16. F. E. Wagstaff, S. D. Rown and I. B. Cutler, Phys. Chem. Glasses 5, (1964).

17. Y. Abe, T. Arahori and A. Naruse, J. Amer. Ceram. Soc. 59, 487 (1976).

18. M. Robinson, R. C. Pastor, R. R. Turk, D. P. Devor, M. Braunstein and R. Braunstein, Mater. Res. Bull. 15, 735 (1980).

19. N. P. Bansal, R. H. Doremus, A. J. Bruce and C. T. Moynihan, J. Amer. Ceram. Soc. 66, 233 (1983).

20. D. Tran (private communication).

21. M. A. Matovich and J. R. A. Pearson, I & EC Fundamentals 8, 512 (1969).

22. F. T. Geyling, Bell Tech. Jl. 55, 1011 (1976).

23. U. C. Paek and C. R. Kurkjian, J. Amer. Ceram. Soc. 58, 330 (1975).

24. L. Kaufman and D. Birnic, Paper 17, Second International Symposium on Halide Glasses, Troy, NY, 1983.

25. P. F. James, J. Mater. Sci. 10, 1802 (1975).

Figure Captions

Figure 1 - Schematic drawing of the three different fiber regions.

Figure 2 - Square root of reduced velocity vs. ten times the reduced axial distance. Fiber is assumed to be at constant temperature.

Figure 3 - Square root of reduced velocity vs. reduced axial distance. Fiber is assumed to be at constant temperature.

Figure 4 - "Same as Figure 3"

Figure 5 - Logarithm of viscosity vs. axial distance.

Figure 6 - Square root of reduced velocity vs. reduced axial distance for constant temperature and cooling fiber.

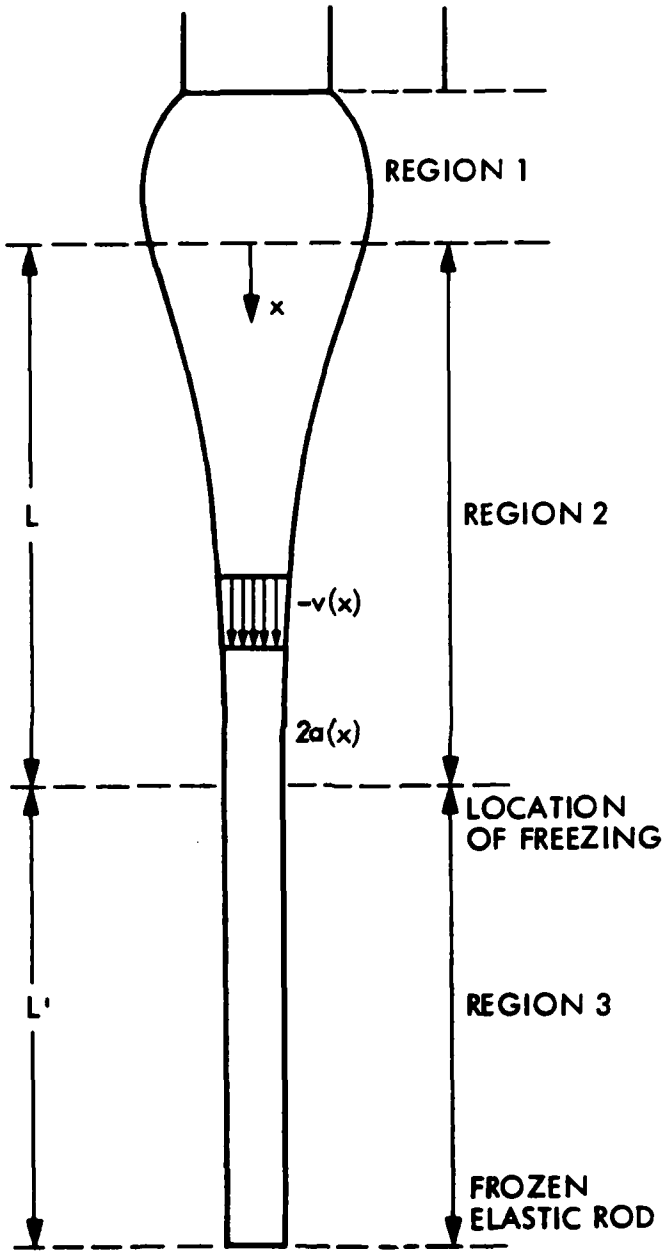
REGION 1
x
L
REGION 2
-v(x)
2a(x)
LOCATION
OF FREEZING
L'
REGION 3
FROZEN
ELASTIC ROD

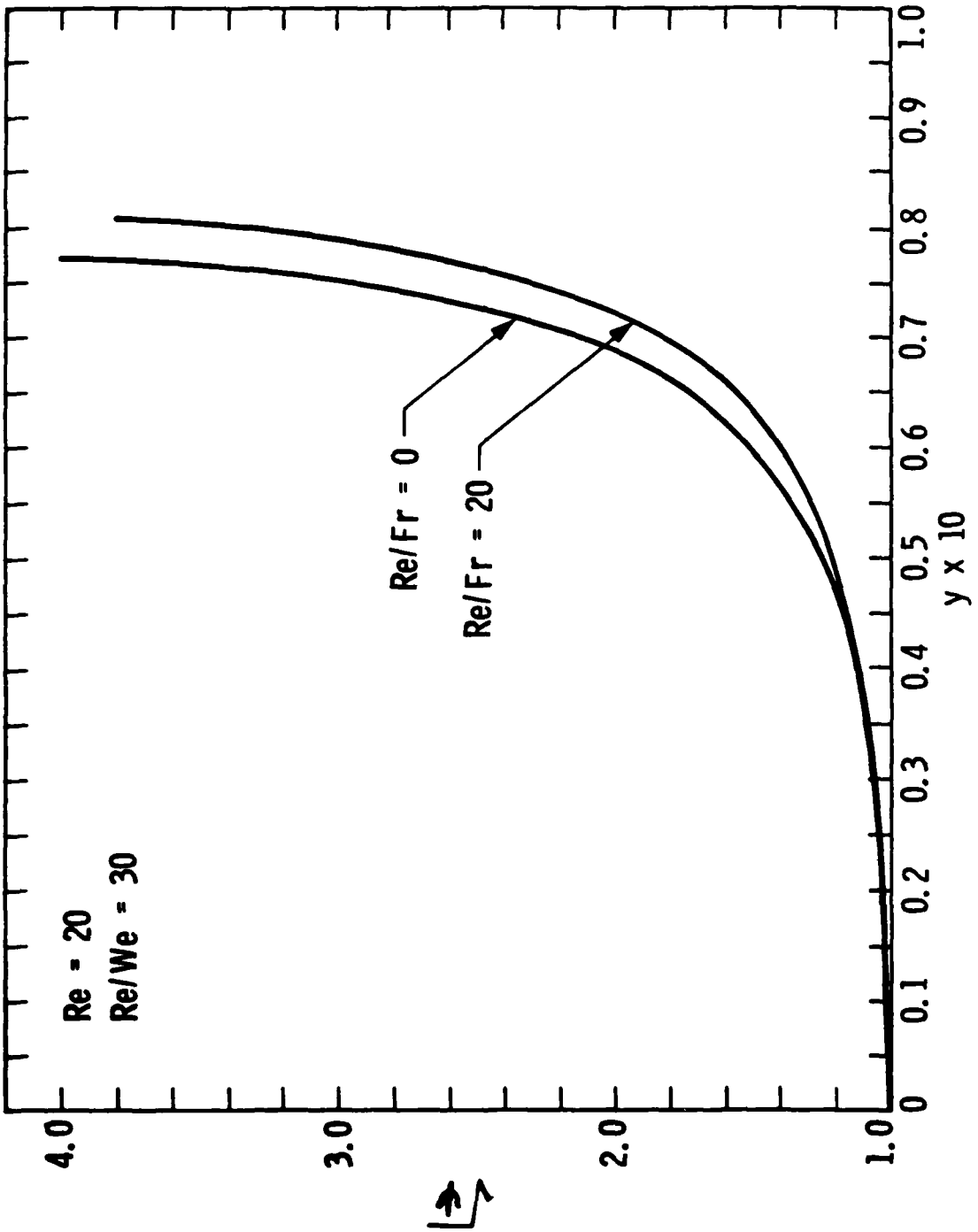
Re = 20
Re/We = 30
Re/Fr = 0
Re/Fr = 20
4.0
3.0
2.0
1.0
0
0.1
0.2
0.3
0.4
0.5
0.6
0.7
0.8
0.9
1.0
y x 10

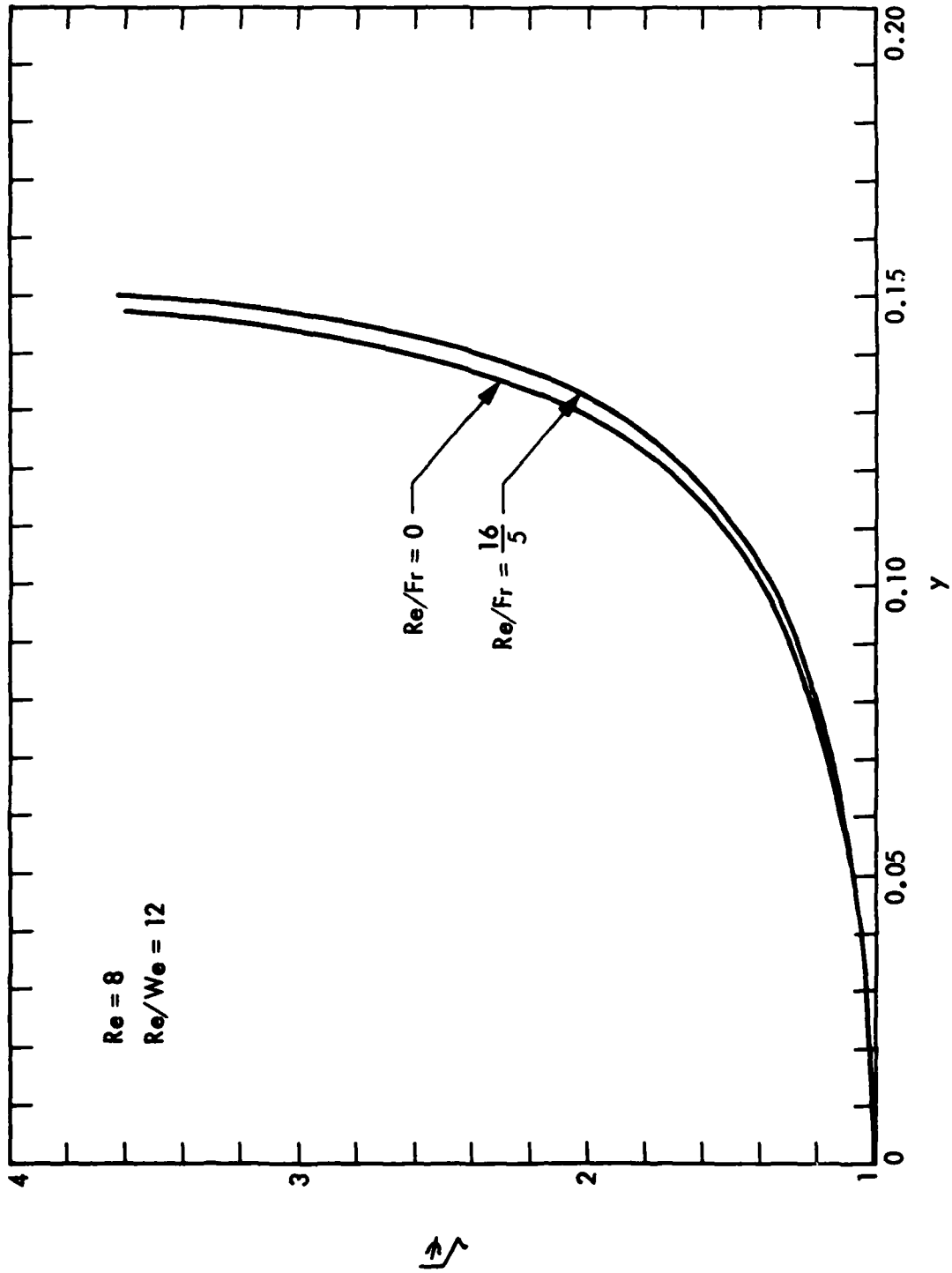
Re = 8
Re/We = 12
Re/Fr = 0
Re/Fr = 16/5
y
0
0.05
0.10
0.15
0.20
1
2
3
4

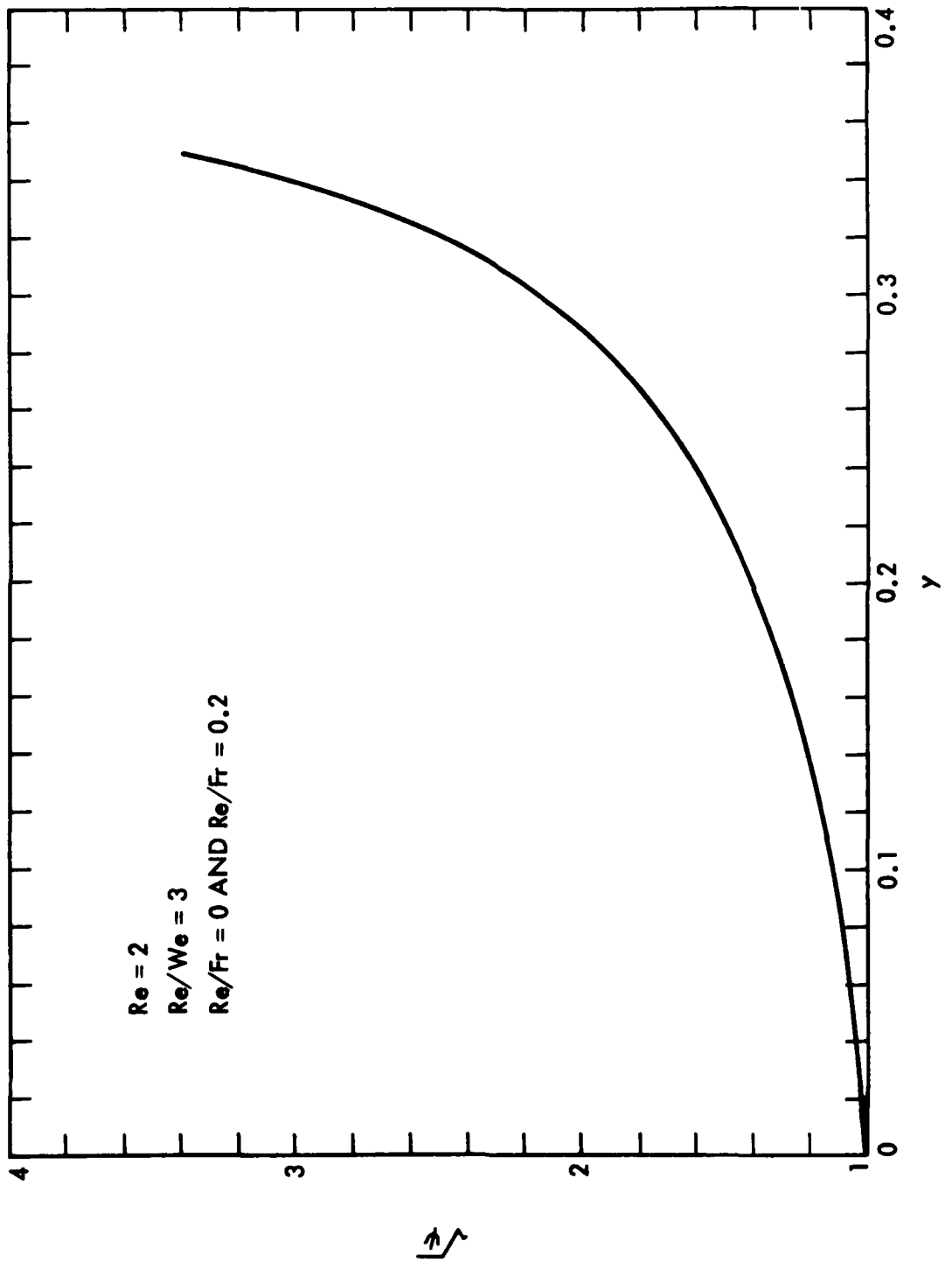
Re = 2
Re/We = 3
Re/Fr = 0 AND Re/Fr = 0.2
0
0.1
0.2
0.3
0.4
y
1
2
3
4
ψ

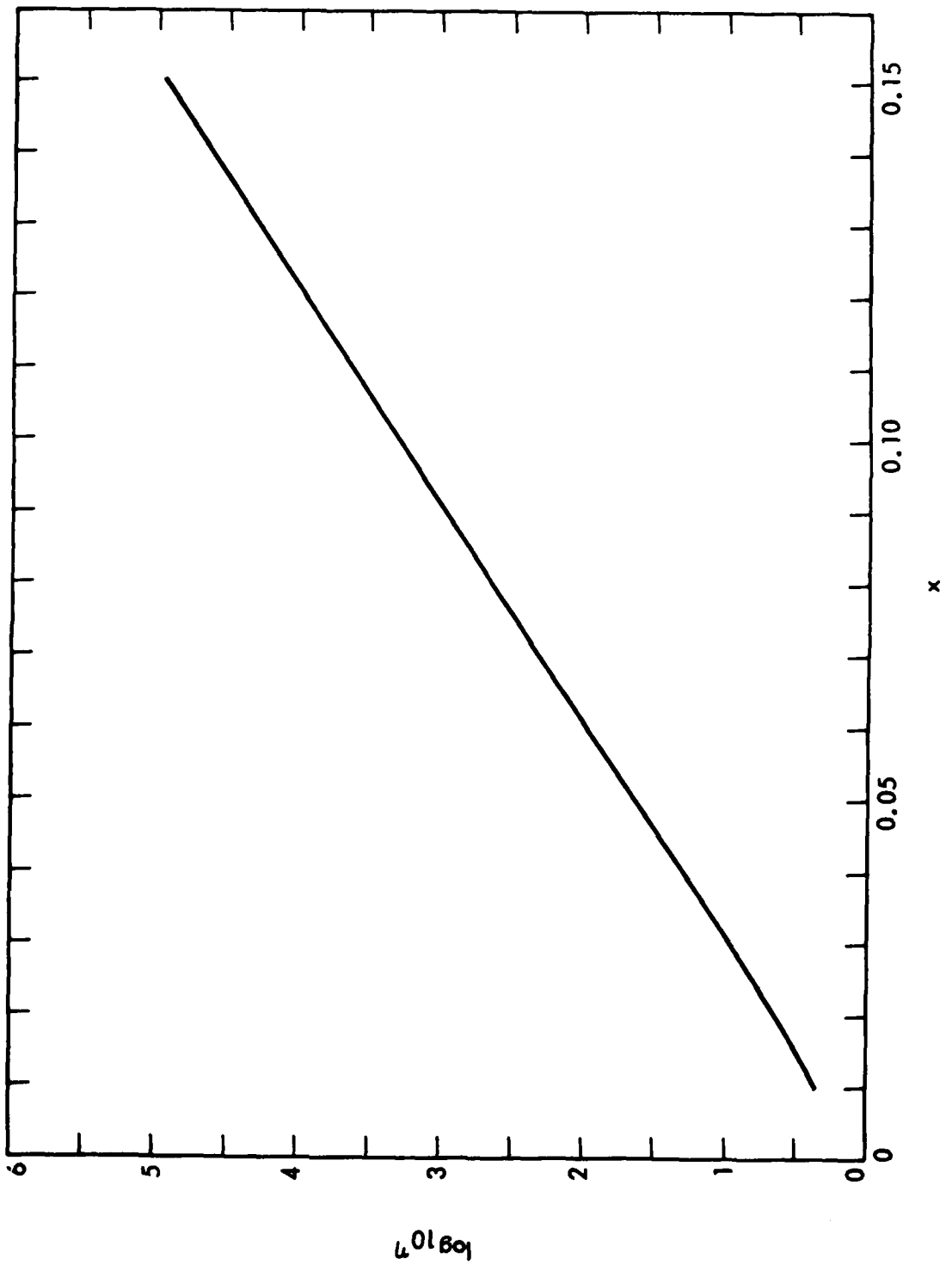
0.15
0.10
0.05
0
x
6
5
4
3
2
1
0
log10η

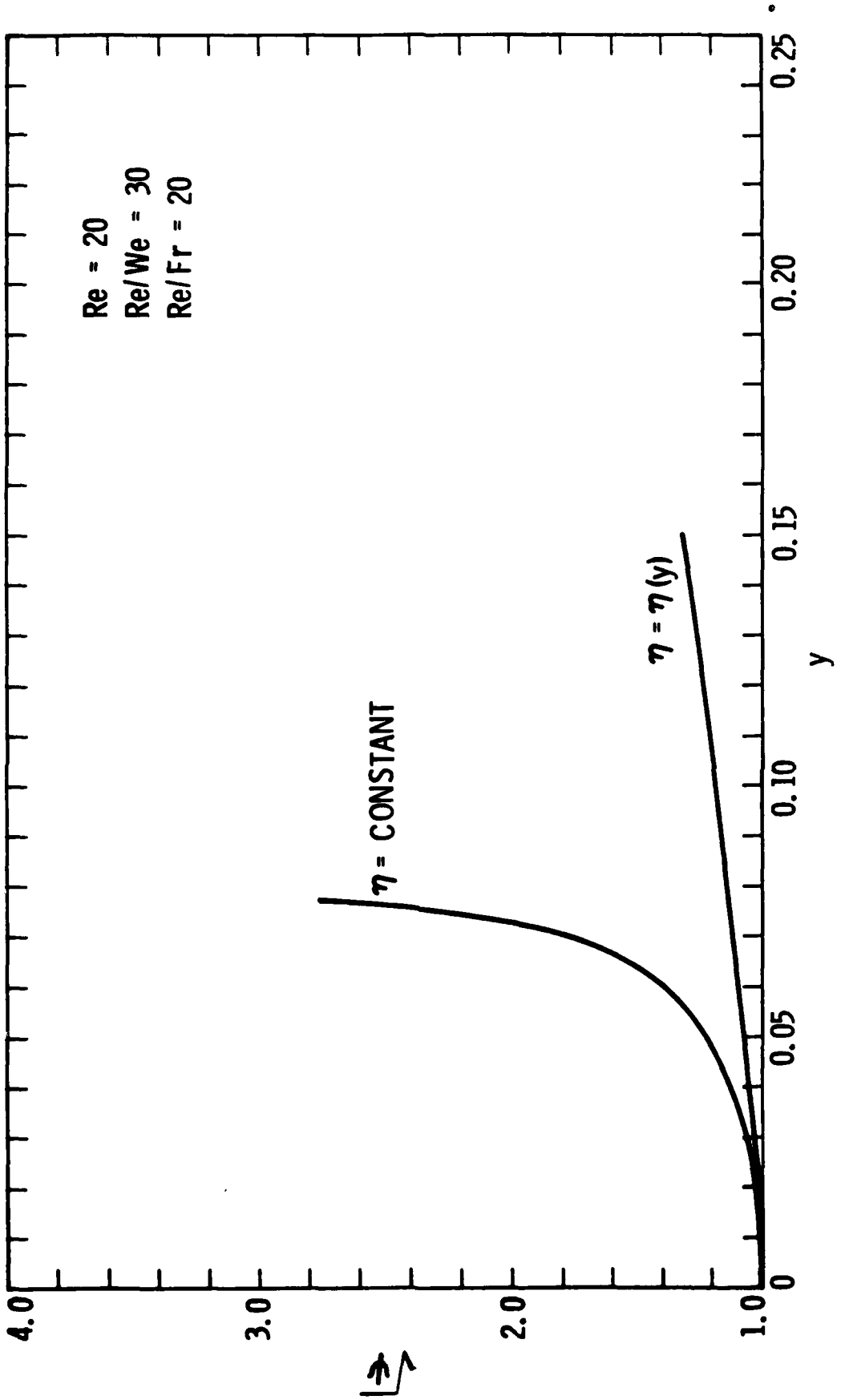
Re = 20
Re/We = 30
Re/Fr = 20
η = CONSTANT
η = η(y)
4.0
3.0
2.0
1.0
η
0
0.05
0.10
0.15
0.20
0.25
y